Low Frequency Ripple Current Compensation with DC Active Filter for the Single-Phase Aeronautic Static Inverter

Zhong Chen, Miao Chen, Yingpeng Luo, Changyou Wang
Aero-Power Sci-Tech Center, College of Automation Engineering
Nanjing University of Aeronautics and Astronautics
Nanjing, 210016, P.R.China
chenz@nuaa.edu.cn

Abstract—**The second order harmonic current drawn by the main part of single-phase aeronautic static inverter which is a typical load in the aircraft power system deteriorates the power quality of aeronautic high voltage power system. In this paper, the low frequency harmonic propagation which is hard to be filtered by the passive components is studied. In order to maintain a good power quality, a DC active power filter (DC-APF) is proposed to be installed in parallel with the aeronautic static inverter, producing the low-frequency current for the load. A novel DC-APF based on the "dual switch" topology is proposed in this paper. This novel configuration is suitable for the aircraft power system with the requirement of high reliability for its inherent "no shoot-through" behavior, optimization of the devices and good comprehensive performance. Control strategy of this con-figuration and discussion about the modeling analysis are given as well. Experimental results are shown to verify the good harmonic compensation characteristic.**

I. INTRODUCTION

The 270V high voltage DC power system becomes a competitive solution for its light weight, easy to realize the uninterruptive supply and high power density [1]. With the increasing use of avionics, the aviation static inverter (ASI) is widely used as the interface circuit of the load in the aircraft DC power system. According to the different switching frequency of isolation stage, two kinds of ASI exist: high-frequency-link type ASI and low-frequency-link type ASI. In this paper, the high-frequency-link type ASI which has lighter weight and two-stage configuration: DC-DC stage and inverter stage is studied.

According to the MIL-STD-704F, voltage ripple of the 270V DC system should be less than 6.0V [2]. The input low-frequency harmonic current drawn by the ASI increases the voltage ripple of the source voltage, leading to the serious harmonic pollution and EMI interference. The deteriorated power quality even will threaten to the safe operation of the aircraft. Therefore, how to deal with the harmonic pollution of the DC power system catches more and more attention.

Passive filter is a traditional method to eliminate the low-frequency harmonic. But the large volume and weight, poor frequency and temperature character and short life make this approach not so popular [3]. Since 80s, active power filters (APF) whose compensation characteristic is not influenced by the system parameters and load condition receive increasing researches and are regarded as the ideal compensation technology [4]. Shunt APF, the most widely used topology, in which small or even no passive components are used could directly be installed in the power system without changing the original configuration and equipment. DC-APF is the APF used in a DC power system, which has been applied in the HVDC [5-6] and low-ripple high-precision dc power supply [7-8]. In the fuel cell based power system, low-frequency ripple current deteriorates the performance and life of the fuel cell. In [9], the coupled inductor is introduced to eliminate the second-order harmonic; in [10], a novel dc active power filtering method based on the center-tap transformer is proposed. No power switches are added, experimental results show that conversion efficiency and performance is increased remarkably.

In this paper, the characteristic of the input current of ASI in the high voltage DC power system is analyzed. A novel topology of DC-APF is proposed, as well as the corresponding control method and system model. In order to verify the feasibility of the proposed harmonic filtering method, a hardware DC-APF prototype is built and tested in the laboratory.

II. INPUT CURRENT ANALYSIS OF SINGLE-PHASE AERONAUTICAL STATIC INVERTER

In this paper, switching function based on the Fourier Series is used to construct the drive signal of the switch devices.

978-1-4577-0541-0/11/$26.00 ©2011 IEEE

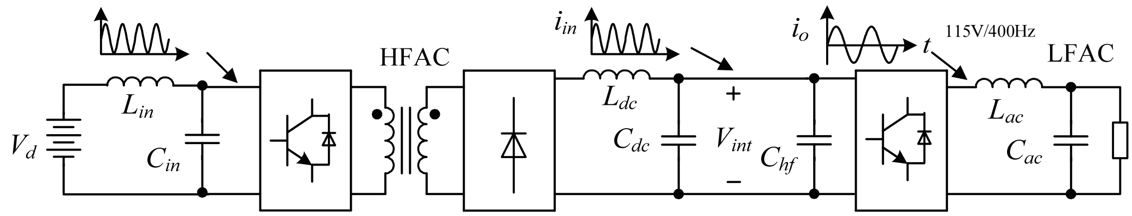

Figure 1. System diagram of the proposed aeronautical active power filter.

Switching function of single phase full bridge inverter with PWM modulation could be expressed as:

$$f(x,y) = M\sin y + \sum_{m=1}^{\infty}\frac{4}{m\pi}J_0(\frac{mM\pi}{2})\sin(\frac{m}{2}\pi)\cos mx + \sum_{m=1}^{\infty}\sum_{n=\pm1,\pm2,\pm3\ldots}^{\infty}\frac{4}{m\pi}J_n(\frac{mM\pi}{2})\sin(\frac{m+n}{2}\pi)\cos(mx+ny-\frac{n\pi}{2}) \quad (1)$$

Here, $x=\omega_c t+\theta_c$, $y=\omega_r t+\theta_r$

ω_c, θ_c are the angle frequency and initial degree of the triangle carrier wave; ω_r, θ_r are the angle frequency and initial degree of the modulation wave; M (=V_r / V_c) is the modulation index, V_c is the peak value of triangle carrier wave, V_r is the peak value of modulation wave.

m=1, 2, 3…, (harmonic order with respect to carrier wave); n=±1, ±2, ±3…, (harmonic order with respect to modulation wave);

J_n(x) refers to the Bessel Function.

Therefore, the input current could be expressed as

$$i_{in}(x,y) = i_o \cdot f(x,y) \quad (2)$$

Here, i_o refers to the output current, and is the function of output voltage u_o and output impedances Z of the inverter.

$$i_o(\omega t) = u_o / Z(\omega t) \quad (3)$$

Meanwhile, u_o is the function of invert input voltage V_{int}.

$$u_o = V_{\text{int}} \cdot f(x,y) \quad (4)$$

After simplifying, the input current is obtained as follow:

$$\begin{aligned} I_{in}(x,y) &= \frac{V_{\text{int}}M^2}{2|Z(\omega_r)|}[\cos(\phi(Z(\omega_r)) - \cos(2y-\phi(Z(\omega_r))] \\ &+ \frac{2V_{\text{int}}M}{|Z(\omega_r)|}\sum_{m=1}^{\infty}\sum_{n=0,\pm1,\pm2,\pm3\ldots}^{\infty}\frac{1}{m\pi}J_n(\frac{mM\pi}{2})\sin(\frac{m+n}{2}\pi) \\ &\cdot[\sin(mx+(n+1)y-\frac{n\pi}{2}-\phi(Z(\omega_r)) \\ &-\sin(mx+(n-1)y-\frac{n\pi}{2}+\phi(Z(\omega_r))] \end{aligned} \quad (5)$$

As (5) shows, the input current consist of four components: the dc component which implies the consumed active power, the second-order low frequency ripple current, the m-order harmonic current respective to the modulation frequency, and bandside harmonic current. Detail analysis is out the scope of this paper. It is noticed that to suppress this second-order low frequency ripple current really requires a large volume of passive filtering components.

III. Configuration and Operation Principle of the Proposed Aeronautical DC-APF

The single-phase high-frequency ASI is illustrated in Fig. 1, which consists of high-frequency inverter, high-frequency transformer, rectifier, inverter, input filter and output filter. The front-end DC-DC converter converts the input dc voltage into the intermediate dc voltage V_{int} needed by the second-stage inverter. An H-bridge inverter topology is used in the second-stage, converting the dc voltage to the 115V/400Hz ac voltage. Input current of the inverter includes dc components, second-order harmonic (800Hz) and high frequency switching components which could be eliminated by the high-frequency capacitor C_{hf} easily. However, the second-order harmonic is hardly compensated by the passive filter, leading to the harmonic propagation in the dc power system. In this paper, a novel DC-APF with high reliability to compensate the input second-order harmonic current is proposed.

A. "Dual Switch" topology based DC-APF

Four exited DC-APF topologies are given in Fig. 2, in which the DC-APF is parallel connected to the dc power system without changing the original circuit configuration. Operation principle is given as follows: load current of ASI i_L consists of the dc component and second-order component. In order to realize the no-ripple current flowing in the source current, a second-order harmonic with the same amplitude but opposite phase angel should be produced by the DC-APF. After the DC-APF's action, source current becomes a pure dc value, while the second-order current is drawn by the DC-APF.

The DC-APF topologies given in Fig. 2(a), (b), (c) have been studied before [11-12]. Topology 1 is proposed to compensate the low-order harmonic current of the 50Hz inverter; topology 2 proposed by Kun X. works as a bus conditioner in the distribution power system; Topology 3 illustrates a conventional dc active filter, which is constructed using a dc chopper and an energy buffer capacitor C. The capacitor C is used as an energy buffer to absorb the ripple power. The inductor L_f can suppress the switching current. However, in the three DC-APFs, the inductors in the dc-link will reduce the efficiency and

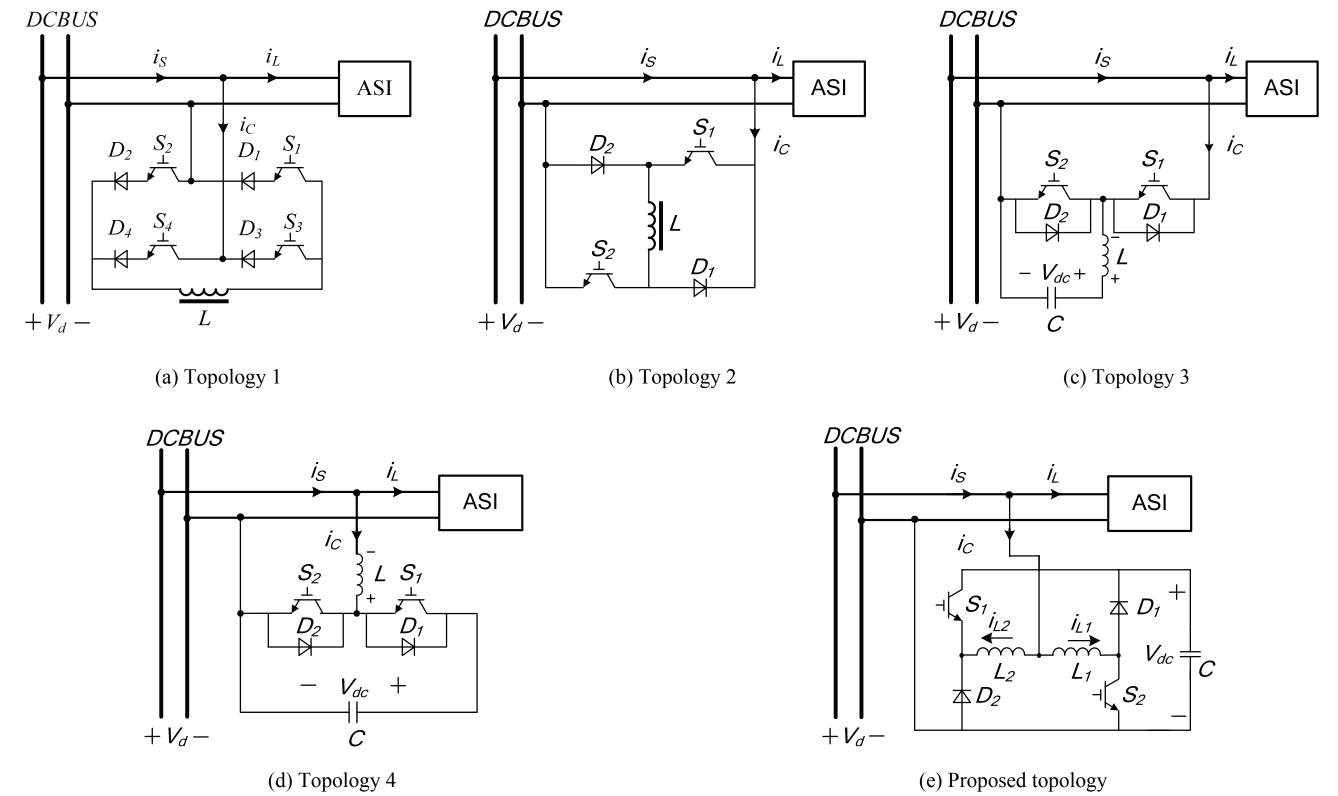

(a) Topology 1 (b) Topology 2 (c) Topology 3

(d) Topology 4 (e) Proposed topology

Figure 2: DC-APF topologies

practicability of the equipment

Another voltage source DC-APF is given in Fig. 2(d). In this configuration, a storage capacitor is connected in the dc-link of the DC-APF, in which the bulky dc reactor is removed from the dc side. Two dual-direction switches work as a dc chopper. However, the potential "shoot-through" of this configuration reduces the reliability of the equipment.

In this paper, a novel DC-APF based on the "dual-switch" configuration is proposed (as shown in Fig. 2(e)). In the proposed topology, a storage capacitor is connected in the dc-link of the DC-APF, each leg is composed of a diode and a power switch. Every power switch works in the "half-cycle" mode, eliminating the possibility of "shoot-through" Each leg connects with the line with its independent inductor L_1 and L_2.

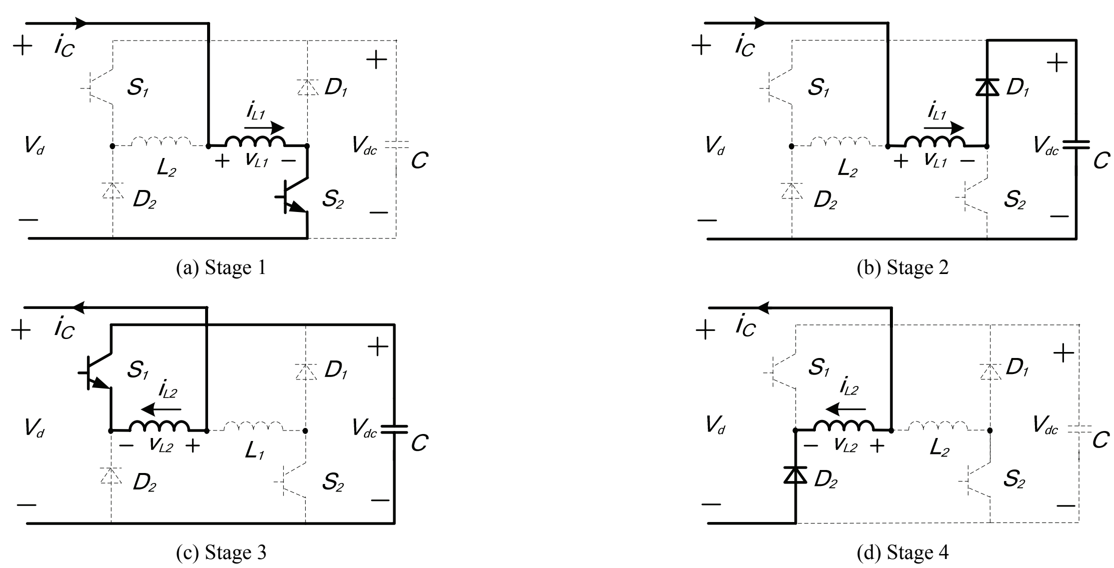

(a) Stage 1 (b) Stage 2

(c) Stage 3 (d) Stage 4

Figure 3: Operation stage of the proposed DC-APF

This novel configuration is suitable for the aircraft power system with the requirement of high reliability for its inherent "no shoot-through" behavior, optimization of the devices and good comprehensive performance.

B. Operation principle of the novel DC-APF

As Fig. 3 illustrates, four different stages exist in the DC-APF. When the compensation current is positive, DC-APF works in the first two stages; when the compensation current is negative, DC-APF works in the last two stages.

Stage 1: The compensation current i_C is positive, power switch S_2 switches on. Considering the voltage between the inductor v_{L1} corresponds to V_d, being positive, the compensation current i_C will be increased (as show in Fig. 3(a)).

Stage 2: The compensation current i_C is positive, power switch S_2 switches off. Diode D_1 becomes conducted for the current's freewheeling. Considering the voltage between the inductor v_{L1} corresponds to V_d-V_{dc}, being negative, the compensation current i_C will be decreased. Moreover, the power system starts to charge the dc capacitor through the diode D_1 (as show in Fig. 3(b)).

Stage 3: The compensation current i_C is negative, power switch S_1 switches on. Considering the voltage between the inductor v_{L2} corresponds to V_d-V_{dc}, being negative, the compensation current i_C will be increased in the negative direction. Moreover, the converter starts to discharge the dc capacitor through the switch S_1 (as show in Fig. 3(c)).

Stage 4: The compensation current i_C is negative, power switch S_1 switches off. Diode D_2 becomes conducted for the current's freewheeling. Considering the voltage between the inductor v_{L2} corresponds to V_d, being positive, the compensation current i_C will be decreased in the negative direction (as show in Fig. 3(d)).

As Fig. 3 illustrates, when the compensation current i_C>0, DC-APF works in the boost state, S_2 or D_1 conducts; when the compensation current i_C<0, DC-APF works in the buck state S_2 or D_1 conducts.

When the switch S_1 or D_1 conducts, the voltage between the inductor could be expressed as:

$$v_L = L\frac{di_C}{dt} = V_d - V_{dc} < 0 \tag{6}$$

When the switch S_2 or D_2 conducts, the voltage between the inductor could be expressed as:

$$v_L = L\frac{di_C}{dt} = V_d > 0 \tag{7}$$

As (3) and (4) show, the voltage between the inductor could be positive or negative in one switching period. So the proposed DC-APF could work as a controlled current source. How to derive the compensation current reference i^*_C fast and accurately and how to generate the compensation current in a high dynamic response play important roles to the DC-APF's compensation performance.

IV. CONTROL STRATEGY AND SYSTEM MODEL

A. Control strategy

Different from traditional APF, compensation current reference extraction in the DC-APF is much easier to be implemented, no complicated harmonic extraction algorithm needed. Here, after the detection of the load current i_L, the dc component of i_L will be derived by using a low pass filter. By abstracting the dc component from the load current, the compensation current reference will be obtained. From above analysis, the current reference is the second-order harmonic component of ASI's input current.

Meanwhile, in order to maintain DC-APF's operation, dc-link voltage should be kept as a constant value. So, the dc-link voltage control loop should be added in the overall control strategy of the DC-APF. After detection of the practical dc-link voltage V_{dc} and comparison with the dc-link voltage reference V_{ref}, the voltage error will be sent to the voltage regulator. Considering the low requirement to the dc voltage control's dynamic response, output of the voltage regulator will attenuated by the coefficient k_n to reduce the voltage control's effect to the compensation current reference.

Finally, the current reference i^*_C is composed of the attenuated voltage control loop's output and the load current's harmonic component.

Based on the above analysis, overall control strategy of the proposed DC-APF under "half-cycle" control mode is given in Fig. 4. Therefore，the error between practical compensation current and current reference will be sent into the hysteresis current controller to generate the PWM drive signal M_1. In fact, from the analysis in Chapter II, only one

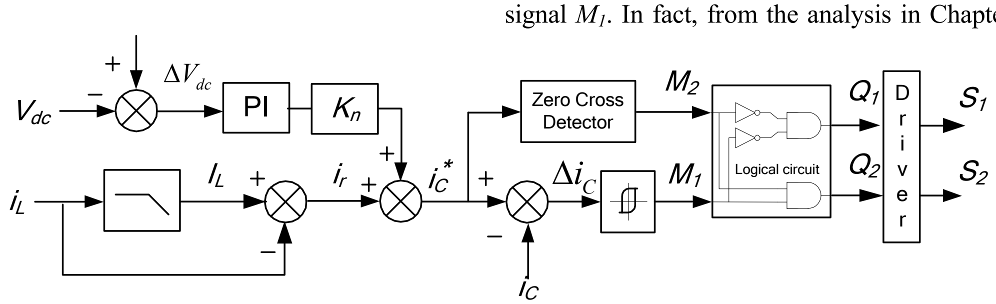

Figure 4. The control scheme of the proposed DC-APF.

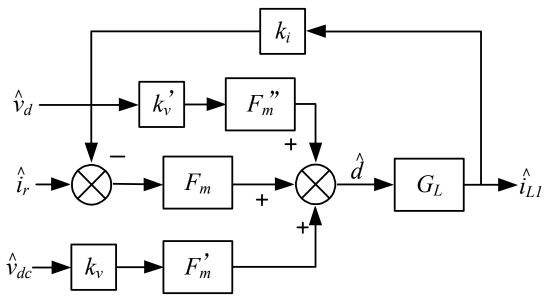

Figure 5: Small signal model of current control loop of boost converter

power switch operates in the half cycle of compensating current, *i.e.* drive signal for S_2 is modulated when $i^*_C>0$, and drive signal for S_1 is modulated when $i^*_C<0$. In order to achieve the "half-cycle" control, polarity of the compensation current' reference will be estimated by using a zero-cross detector to derive a polarity control signal M_2. Final drive signals Q_1 and Q_2 will be obtained from the logical circuit with the input of M_1 and M_2.

B. *Modeling and analysis*

The hysteretic current control has been modeled in former research [13, 14]. Therefore, the small signal model of boost mode converter will be obtained (as shown in Fig.5). Here, k_i corresponds to the detection coefficient of the inductor current i_L, k_v and k_v' correspond to the detection coefficient of the dc-link voltage v_{dc} and DC bus voltage.

Where

$$\frac{\hat{d}}{\hat{i}_r}=F_m=\frac{-2L}{V_{dc}T_s k_i} \tag{8}$$

$$\frac{\hat{d}}{\hat{v}_{dc}}=k_v F_m'=\frac{1-D}{V_{dc}} \tag{9}$$

$$\frac{\hat{d}}{\hat{v}_d}=k'_v F''_m=-\frac{1}{V_{dc}} \tag{10}$$

$$G_L(s)=\frac{\hat{i}_{L1}(s)}{\hat{d}(s)}\approx\frac{V_{dc}}{sL} \tag{11}$$

Therefore, transform function of the hysteresis current control loop could be expressed as:

$$\begin{aligned}\frac{\hat{i}_{L1}(s)}{\hat{i}_r(s)}&=\frac{F_m(s)G_L(s)}{1+F_m(s)G_L(s)k_i}=\frac{\frac{V_{dc}}{sL}\cdot\frac{\hat{d}(s)}{\hat{i}_r(s)}}{1+\frac{\hat{i}_L(s)}{\hat{d}(s)}\cdot\frac{\hat{d}(s)}{\hat{i}_r(s)}\cdot k_i}\\&=\frac{\frac{2}{k_i T_s s}}{-1+\frac{2}{T_s s}}\approx\frac{1}{k_i}\end{aligned} \tag{12}$$

So, as (12) shown, when the switching frequency is high enough, the hysteretic current control loop could be

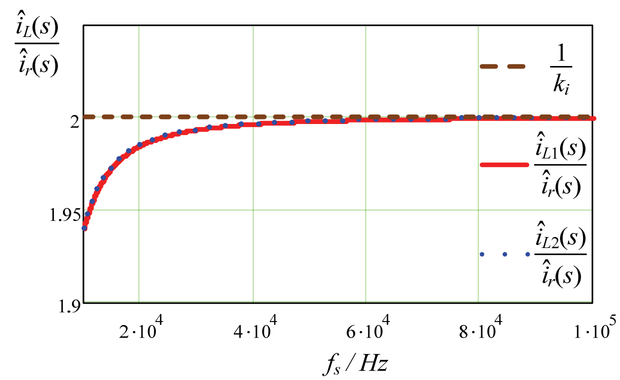

Figure 6 Frequency characteristic of hysteretic current control loop in the boost / buck converter.

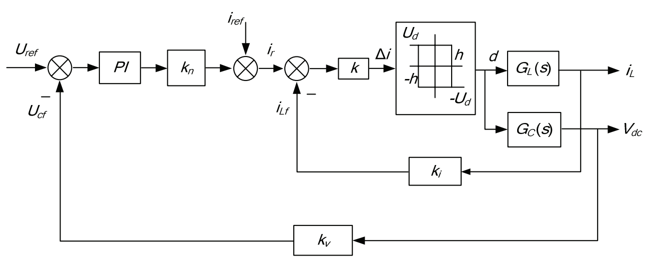

(a) overall control diagram

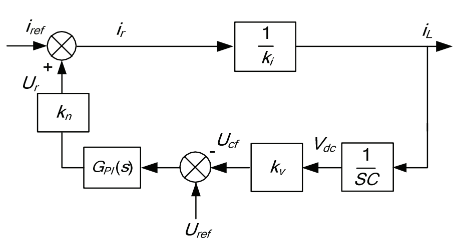

(a) equivalent control diagram in the first state

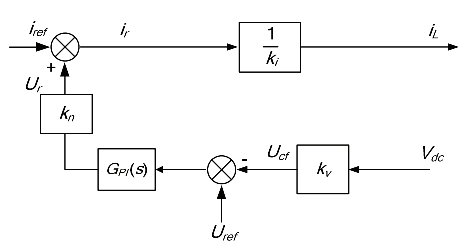

(b) equivalent control diagram in the second state

Figure 7: System control diagram and its equivalents.

regarded as a proportional block. Similar conclusion could be induced for the small signal analysis of buck mode (as shown in Fig. 6). In the Fig. 6, the solid and dot curves imply the practical frequency characteristics of boost and buck converter, and dash line is the equivalent linear controller. Consistent with former analysis, these three curves overlap in high switching frequency.

The overall system control diagram is illustrated in Fig. 7(a). Based on the equivalent model of the hysteretic current controller, two distinguished equivalent control model are deduced for two different working modes of DC-APF (as shown in Fig. 7(b) and (c)).

In the first mode including the stage 2 and 3 of Fig. 3, compensation current flows through the dc-link capacitor, the overall system operates in a open-loop way. As we all known, there is no instability problem for the system with open-loop control strategy.

In the second mode including the stage 1 and 4 of Fig. 3, compensation current does not affect the dc-link voltage, the overall system operates in a close-loop way. In this close-control mode, transfer function could be expressed as:

$$\frac{i_L(s)}{i_{ref}(s)} = \frac{Cs^2}{k_i Cs^2 + k_v k_n k_{Vp} s + k_v k_n k_{Vi}} \tag{13}$$

Here, the voltage regulator could be expressed as:

$$G_{PI}(s) = k_{Vp} + k_{Vi} / s \tag{14}$$

By using the Routh's Criterion, all the indexes of the characteristic equation should be positive, *i.e.* $k_iC>0$ and $k_vk_nk_{Vp}>0$, which is very easy to be implemented in the practical application. Therefore, the novel DC-APF with current hysteretic control is very stable.

V. EXPERIMENTAL RESULTS

In order to verify the feasibility of above analysis and proposed topology, two hardware prototypes are built and tested in the laboratory. One is a 400Hz ASI with PWM control and 1kVA power capacity. The other is the proposed DC-APF for the low-frequency ripple compensation of the ASI. Specifications of the APF prototype are given as follows: ac interface inductor is as large as 800uH; the dc-link capacitor is selected as 1000uF; dc-link voltage is 400V.

Fig. 8(a) shows the output voltage and output current of the 400Hz ASI. Fig. 8(b) shows waveforms and spectrums of the input current. As Fig. 8 shown, a large number of second-order harmonic and PWM switching harmonic components exist in the input current of ASI.

Fig. 9 shows the picture of the DC-APF system, containing the DC bus capacitors, the input filters of ASI, PWM inverter, output filters, and the proposed "Dual Switch" DC-APF.

Fig. 10(a) shows drive signals of two Mosfets, which are working in the "half-cycle" mode. Fig. 10(b) shows current waveforms of two inductors, in which the currents only flow in one direction.

Fig. 11 shows the key current waveforms of the proposed DC-APF under no load and full load conditions. In the no-load condition, DC-APF acts as a reactive power generator, reactive power is circuiting between the ASI and

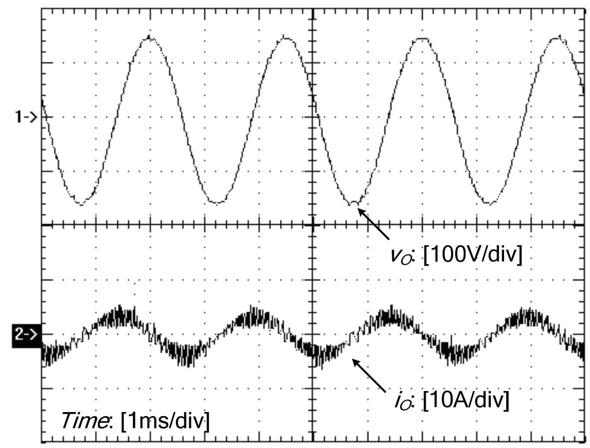

(a) Output voltage and output current

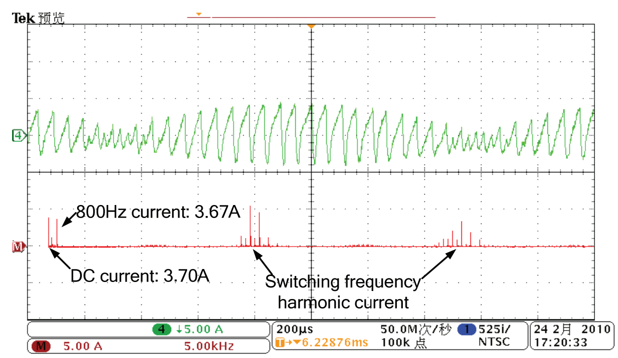

(b) Input current waveforms and its spectrum

Figure 8: Key experimental waveforms of the ASI.

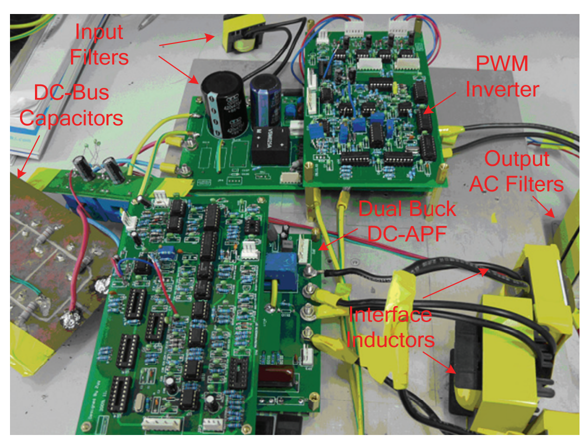

Figure 9: Picture of the novel DC-APF prototype

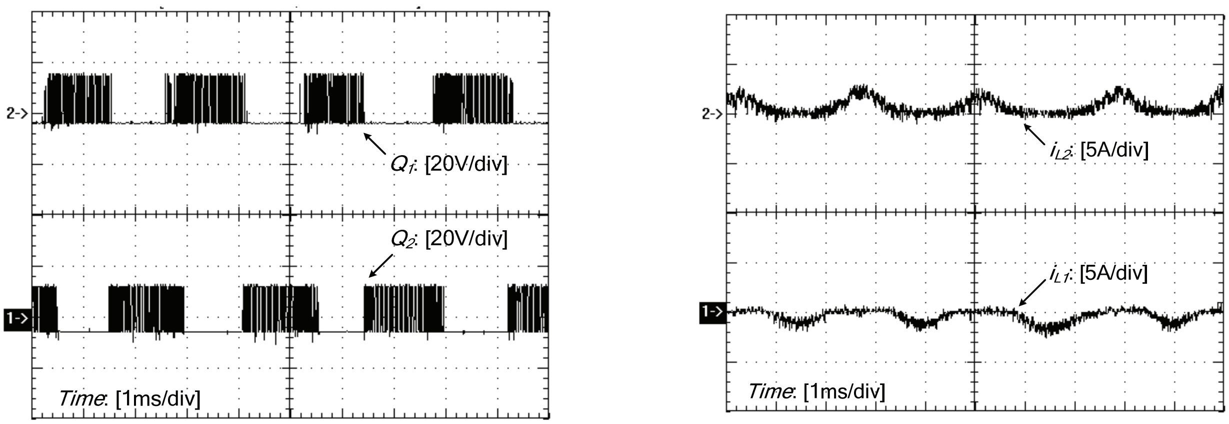

(a) PWM drive signals

(b) Currents of the inductors

Figure 10: Drive signal and inductor current waveforms of the "Dual-Switch" DC-APF.

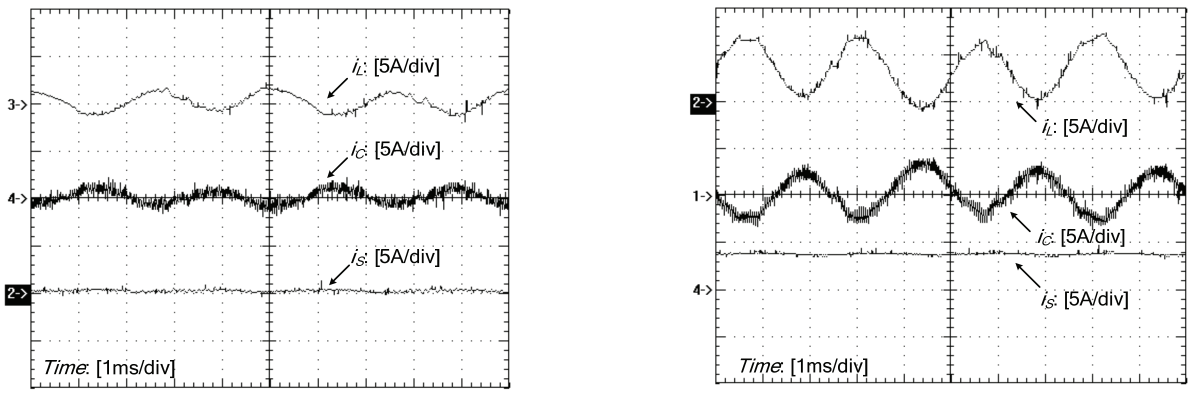

(a) Experimental current waveforms under no load

(b) Experimental current waveforms under full load

Figure 11: Key waveforms of the DC-APF system.

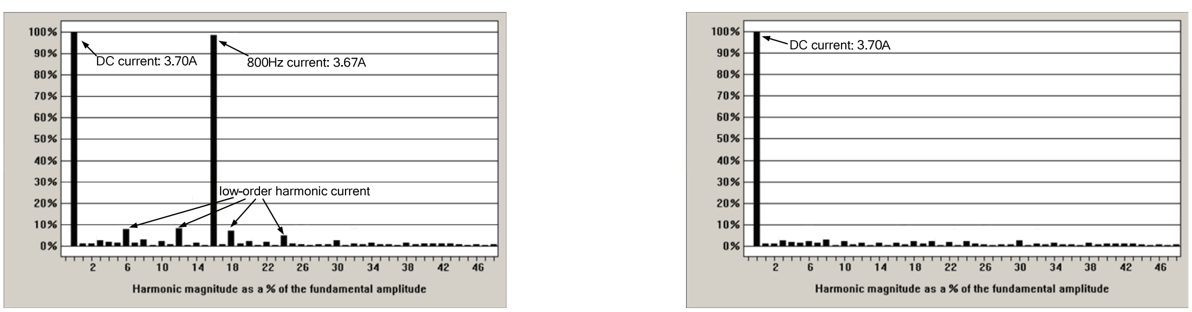

(a) Source current spectrum without DC-APF

(b) Source current spectrum with DC-APF

Figure 12: Source current spectrum of the DC-APF system.

DC-APF, no power is supplied by the grid except the power losses. After the DC-APF's operation, the source current becomes nearly zero (as shown in Fig. 11(a)). In the full load, a number of active powers are supplied to the load from the grid, while the reactive power is supplied by the DC-APF (as shown in Fig. 11(b)).

Meanwhile, the low frequency harmonic current generated by the three-phase diode rectifier based DC power supply have been compensated as well (as shown in Fig. 12). After the DC-APF's operation, only the dc component of the load current is left in the source current.

VI. Conclusion

In this paper, the generation and propagation behavior of second-order harmonic component of the ASI input current are studied. A novel DC-APF based on the "Dual-switch" topology is proposed to compensate the low frequency ripple current. This novel configuration under current hysteretic control is advanced for its simple construction, easy implementation to control and good compensation performance. Moreover, the overall system model is built to show a good stability of the novel configuration. Experimental results with good compensation performance are shown to confirm the feasibility of the DC-APF and above analysis.

ACKNOWLEDGMENT

This work was supported by the National Nature Science of China under Award 51007037, Research Fund for the Doctoral Program of Higher Education of China under Award 200802871033, Aeronautical Science Foundation of China under Award 2009ZC52030 and the NUAA Research Funding under Award NS2010062 and NJ2010015.

REFERENCES

[1] J. A. Rosero, J. A. Ortega, E. Aldabas, and L. Romeral, “Moving towards a more electric aircraft,” IEEE Aerosp. Electron. Syst. Mag., vol.22, no. 3, pp. 3-9, Mar. 2007.

[2] Aircraft Electric Power Characteristics. Military Standard, MIL-STD-704F, 2004.

[3] D. C. Hamill, “An efficient active ripple filter for use in dc-dc conversion,” IEEE Trans. Aerosp. Electron. Syst., vol. 32, no. 3, pp. 1077-1084, 1996.

[4] H. Akagi, Y. Kannazawa, and A. Nabae, “Instantaneous reactive power compensators comprising switching devices without energy storage components” IEEE Trans. Ind. Appl., vol. IA-20, no. 3, pp. 625-630, May 1984.

[5] W. Zhang, G. Asplund, A. Aberg, U. Jonsson and O. Loof, “Active DC filter for HVDC system-a test installation in the Konti-Skan DC link at Lindome converter station”, IEEE Transactions on Power Delivery, vol. 8, no. 3, pp. 1599-1606, May 1993.

[6] A. J. V. Miller, and. M. B. Dewe, “Harmonic measurements made on the upgraded New Zealand inter-island HVDC transmission system,” IEEE Transactions on Power Delivery, vol. 9, no. 3, pp. 1281-1288, July 1994.

[7] K. Li, J. Liu, G. Xiao, and Z. Wang, “Novel load ripple voltage-controlled parallel DC active power filters for high performance magnet power supplies,” IEEE Transactions on Nuclear Science, vol. 53, no. 3, pp. 1530-1539, 2006.

[8] A. C. Chow, andD. J. Perreault, “Design and evaluation of a hybrid passive/active ripple filter with voltage injection” IEEE Trans. Aerosp. Electron. Syst., vol. 39, no. 2, pp. 471-480, 2003

[9] R. S. Gemmen, “Analysis for the effect inverter ripple current on fuel cell operating condition” J. Fluids Eng., vol. 125, no. 3, pp. 576-585, Nov. 2003.

[10] S. K. Mazumder, R. K. Burra, and K. Acharya, “A Ripple-Mitigating and Energy-Efficient Fuel Cell Power-Conditioning System,” IEEE Transactions on Power Electronics, vol. 22, no. 4, pp. 1437-1452, 2007.

[11] Kun Xing, Modeling, analysis and design of distributed power electronics system based on building block concept, Blacksburg, Virginia, Virginia Polytechnic Institute and State University, 1999.

[12] J. Itoh and F Hayashi, “Ripple Current Reduction of a Fuel Cell for a Single-Phase Isolated Converter Using a DC Active Filter with a Center Tap,” IEEE Transactions on Power Electronics, vol. 25, no. 3, pp. 550-556, March 2010.

[13] J. H. Park and B. H. Cho, “mall signal modeling of hysteretic current mode control using the PWM switch model,” Proc. IEEE COMPEL Workshop, Troy, New York, USA, 2006: 225-230.

[14] J. Wang, L. Liu, F. Zhang, C. Gong and Y. Ma, “Modeling and Analysis of Hysteretic Current Mode Control Inverter,” Proc. IEEE APEC 2009, Washington, DC, USA, 2009: 1338-1343.